

Compartmentalization, Intracellular Transport, and Autophagy of Tomato Spotted Wilt Tospovirus Proteins in Infected Thrips Cells

Diane E. Ullman, Daphne M. Westcot, Kelly D. Chenault, John L. Sherwood, Thomas L. German, Murali D. Bandla, Frank A. Cantone, and Helen L. Duer

First author: Department of Entomology, University of California, Davis, California 95616; second author: Department of Entomology, University of Hawaii, 3050 Maile Way Rm 310, Honolulu 96822; third, fourth, sixth, and eighth authors, Department of Plant Pathology, Oklahoma State University, Stillwater 74078; fifth author: Department of Plant Pathology, University of Wisconsin, Russell Laboratories, 1630 Linden Dr., Madison 53706.

F. A. Cantone's present address: Boyce Thompson Institute, Cornell University, Ithaca, NY 14853.

Send correspondence to D. E. Ullman.

This research was supported by the USDA under CSRS Special Grant 91-34135-6138 managed by the Pacific Basin Advisory Group, USDA Competitive Grant 91-37302-6295, Biomedical Research Support Grant, University of Hawaii-Manoa, Research Centers in Minority Institutions Grant RR-03061 from National Institutes of Health and project H-2022 of the Oklahoma Agricultural Experiment Station. This is journal series 4060 of the Hawaii Institute of Tropical Agriculture and Human Resources.

We thank D. Gonsalves for polyclonal antibody to the TSWV 78 kDa membrane glycoprotein (G1), M. Wang and J. Cho for polyclonal antibody to purified TSWV, and R. Allen, T. Weatherby, and M. Dunlap for technical assistance and use of the University of Hawaii Pacific Biomedical Research Center's Biological Electron Microscope Facility.

Accepted for publication 6 February 1995.

ABSTRACT

Ullman, D. E., Westcot, D. M., Chenault, K. D., Sherwood, J. L., German, T. L., Bandla, M. D., Cantone, F. A., and Duer, H. L. 1995. Compartmentalization, intracellular transport, and autophagy of tomato spotted wilt tospovirus proteins in infected thrips cells. *Phytopathology* 85:644-654.

Tomato spotted wilt tospovirus (TSWV) replicates in at least one of its thrips vectors, *Frankliniella occidentalis*. Viral proteins accumulate in cytoplasmic inclusions, but the location and composition of these inclusions have not been fully elucidated. Observations by electron microscopy of TSWV-infected thrips cells immunolabeled with antibodies to TSWV nucleocapsid protein (N), the membrane glycoproteins (G1 or

G2), and the nonstructural protein encoded by the S RNA (NSs) indicated that TSWV encoded proteins were compartmentalized within viroplasm, dense masses, amorphous inclusions, and paracrystalline arrays. Amorphous inclusions have not been previously reported in TSWV infected tissues. Viral proteins were immunolocalized in structures known to be involved in intracellular transport and degradation of proteins including vesicles, putative autophagic vacuoles, and residual bodies. This is the first account of immunolocalization of TSWV-encoded proteins at intercellular membranes and membranes thought to be part of the Golgi complex.

Additional keyword: detection.

Tomato spotted wilt tospovirus (TSWV) is the type member of the genus *Tospovirus*, the only genus in the family *Bunyaviridae* containing viruses that infect plants (5,12,25,32). Severe pandemics in food, fiber, and ornamental crops have been caused by tospoviruses (17,25) and have received international attention. The genome of TSWV consists of two ambisense RNA segments, small (S) and middle (M) (13,19,21), and the large (L) RNA that is negative sense (1,11,17). The S RNA of TSWV encodes the viral nucleocapsid protein (N) and a nonstructural protein (NSs) found in fibrous paracrystalline inclusions in infected insect and plant cells, but not in assembled virions or healthy plants (10,13,18,20,36,37,39,43). The M RNA encodes a precursor to the two glycoproteins (G1 and G2) that are associated with the viral membrane and a nonstructural protein (NSm) that is the putative movement protein (9,19,21). The L RNA encodes a protein that is the viral RNA polymerase (1,11,17). Electron microscope studies of TSWV infected plants have shown that TSWV is present in many cell types (16). Electron microscopy studies show configurations within viroplasms and in the Golgi body that have been interpreted as membranes budding to form particles (24). Double-enveloped particles and presence of paired parallel membranes have also been reported (18,24). The association and role of these structures in TSWV replication has not been confirmed with serologically specific electron microscopy.

TSWV replicates in its thrips vectors (36,43) and is persistently transmitted from plant to plant by several thrips species (order: Thysanoptera) (17). Several types of cytoplasmic inclusions have been identified in tospovirus-infected insect and plant cells (18, 20,36,37,39,42,43) although the specific protein composition of these inclusions has not been completely identified. In plants, TSWV and impatiens necrotic spot tospovirus (INSV) N proteins are associated with dense masses (39) (nucleocapsid accumulations [NCA]) (18,20) that occur in the cytoplasm or embedded in viroplasm (18,20,39). Similar inclusions occur in insect cells, except that dense masses are most often embedded in viroplasm and are only rarely found occurring in the cytoplasm (36,37,43). In plants and insects, fibrous paracrystalline arrays of various shapes are associated with NSs (18,20,36,37,43). This protein may also be found distributed in the cytoplasm of infected plant and insect cells (20,43).

Amorphous inclusions have been reported in plant cells infected with INSV (39), but have not previously been reported in plant or insect cells infected with TSWV. Amorphous inclusions associated with INSV-infected plants did not label with polyclonal antibodies to INSV N or G2 proteins (39). Previously, tospovirus glycoproteins have only been found in the membrane of assembled virions and have not otherwise been immunolocalized in either plant or insect cells. Cell response to accumulation of TSWV-encoded proteins has not been studied nor have the processes surrounding virion translocation and maturation in infected

plant and insect cells been fully elucidated. Vertebrate and invertebrate cells respond to accumulated endogenous and exogenous proteins with an autophagic system that involves controlled autolytic elimination of organelles, inclusions, and foreign proteins (15). This intracellular digestive system is involved in normal cell renewal and responds to altered states of physiological activity, such as virus infection (15,27). The role of this system in responding to infection with plant viruses has not been elucidated in insect cells. In this paper, we report the localization of TSWV N, G1, G2, and NSs proteins in infected thrips cells, provide the first serological evidence that N, G1, and G2 can be found at intercellular membranes and membranes thought to be part of the Golgi complex, and show that N, G1, G2, and NSs proteins are compartmentalized in cytoplasmic inclusions. The hypothesis that TSWV-encoded proteins are transported intracellularly and may enter the cell's autophagic system is discussed.

MATERIALS AND METHODS

Plant Material and Virus Isolate. A thrips-transmissible TSWV isolate collected from tomato on the Hawaiian island of Maui (TSWV-MT2) was used for all serological tests and for thrips acquisition. The isolate was maintained by inoculation with the western flower thrips (WFT), *Frankliniella occidentalis* (Pergande), as previously described (35). Infected *Emilia sonchifolia* L. plants were maintained as thrips acquisition hosts in greenhouses at the University of Hawaii-Manoa campus. TSWV-MT2 was used to mechanically inoculate *Datura stramonium* L. plants that were then used for virus purification (36).

Insects. The WFT colony used in these studies has been previously described (23,35). The colony was maintained on pods of *Phaseolus vulgaris* cv. Green Crop as previously described (35).

Antibodies. Polyclonal antibody indicated to be specific to the TSWV 78 kDa membrane glycoprotein (G1) was provided by Dennis Gonsalves at Cornell University (40). A monoclonal antibody to the TSWV 58 kDa membrane glycoprotein (G2) was produced using G2 isolated from sodium dodecyl sulfate-polyacrylamide gel electrophoresis (SDS-PAGE) gels of purified virions as previously described (2,34). Western blot analysis showed that this antibody reacted to a band of 58 kDa from infected plant tissue and not to healthy plant extracts (data not shown). Polyclonal antibody to purified TSWV was provided by Min Wang and John Cho, University of Hawaii. We produced anti-NSs antibody as previously reported (36). Antibodies to the TSWV N protein were produced as follows. The TSWV N gene was subcloned from a Bluescript vector into the vector pET 14b using polymerase chain reaction (PCR) as previously described (36). Primers complementary to the 5' or 3' end of the N gene were designed with the appropriate restriction enzyme site sequences

TABLE 1. Comparison of mean gold label per cm² on viroplasm and dense masses, amorphous inclusions, paracrystalline arrays, and cytoplasmic regions in thin sections of noninfected and tomato spotted wilt tospovirus (TSWV)-infected larval *Frankliniella occidentalis* (Pergande)^a

Cell Regions	Treatments			Rabbit serum
	Anti-N	Anti-G1	Anti-NSs	
Viroplasm and dense masses	12.02 ^b	0.16	0.02	0.02
Amorphous inclusions	0.11	13.52 ^b	0.05	0.27
Paracrystalline arrays	0.10	0.10	7.28 ^b	0.18
Cytoplasm, infected insects	0.19	0.08	0.11	0.25
Cytoplasm, noninfected insects	0.16	0.27	0.05	0.22

^a Measurements were made in midgut epithelial cells reacted with polyclonal antibodies raised against TSWV nucleocapsid protein (N), TSWV 78 kDa membrane glycoprotein (G1) and the nonstructural protein (NSs) encoded by the small RNA segment of TSWV.

^b Mean gold label per cm² is significantly higher than on other structures or cytoplasm of noninfected and TSWV-infected insects ($P < 0.0001$).

for insertion into pET 14b. The N gene was expressed in *E. coli* BL21 (DE3) (Novagen, Madison) and purified using denaturing conditions with the Novagen His-Tag system. The purified protein was used for the production of polyclonal antisera by methods similar to those previously described (36). Western blot analysis showed that the polyclonal serum to the N protein reacted with a band of 29 kDa in both infected plant tissue and induced *E. coli* protein extracts (data not shown). No cross-reactivity with healthy plant tissue or uninduced *E. coli* proteins was observed.

Immunocytochemistry. Dissected WFT organs used for immunocytochemical analyses were fixed and embedded in LR-White resin as previously described (42). Insects for these tests were subsampled from acquisition and transmission experiments (see next section for description). Embedded samples were serially sectioned at 90 to 100 nm and placed on nickel or copper formvar coated slot grids. Serial sections were then incubated at room temperature with 5% fetal bovine serum in 0.05 M phosphate buffered saline with 0.02 M glycine (pH 7.4) (FBS-PBS-GLY) for 5 min and reacted with anti-N (1:10 in 5% FBS-PBS-GLY), anti-G1 or G2 (1:10 in 5% FBS-PBS-GLY) or anti-NSs polyclonal antibody (1:10 in 5% FBS-PBS-GLY) for 40 min. Grids reacted with anti-N or anti-G1 antiserum were labeled with 10, 15 or 20 nm Protein A-Gold (1:15 in 5% FBS-PBS-GLY). Those reacted with anti-NSs antiserum were labeled with 15 nm gold-conjugated goat-anti-rabbit antiserum (GAR) (1:15 in 5% FBS-PBS-GLY) and those reacted with anti-G2 were reacted with rabbit-anti-mouse (1:1,000 5% FBS-PBS-GLY) and labeled with 15 nm Protein A-Gold (1:15 in 5% FBS-PBS-GLY). Serum controls included sections from virus infected individuals incubated with normal rabbit serum (1:10 in FBS-PBS-GLY) when polyclonal antibodies were used and normal mouse serum (1:10 in FBS-PBS-GLY) when monoclonal antibodies were used. These sections were then tested for reaction to the appropriate gold conjugates. Sections from noninfected individuals fed on sucrose or healthy plants were also labeled with each polyclonal antibody or rabbit serum. Washes were done in PBS and grids were fixed with 2% glutaraldehyde in distilled water, washed with distilled water, stained with 5% uranyl acetate in distilled water and lead citrate, and viewed with a Zeiss 10A electron microscope. Immunolabel-

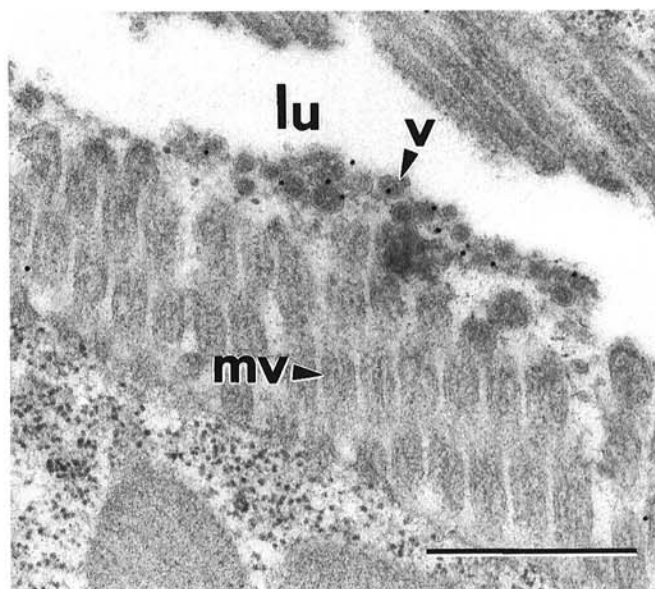


Fig. 1. Electron micrograph of a thin section of the lumen of a larval thrips midgut epithelial cell. Virions ingested from an infected plant are labeled with polyclonal antibody to the tomato spotted wilt tospovirus 78 kDa membrane glycoprotein (G1) and 15 nm Protein A-gold. Bar = 1 μ m. lu, lumen; mv, microvilli; v, virions.

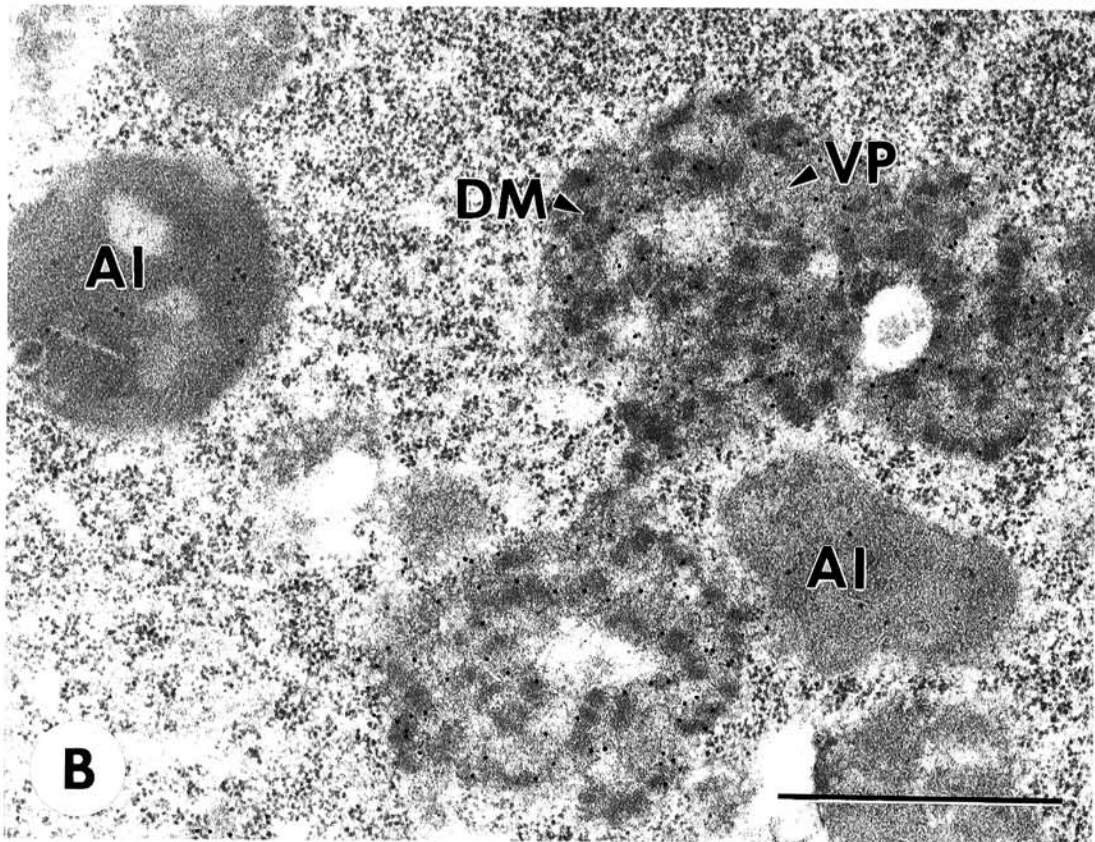
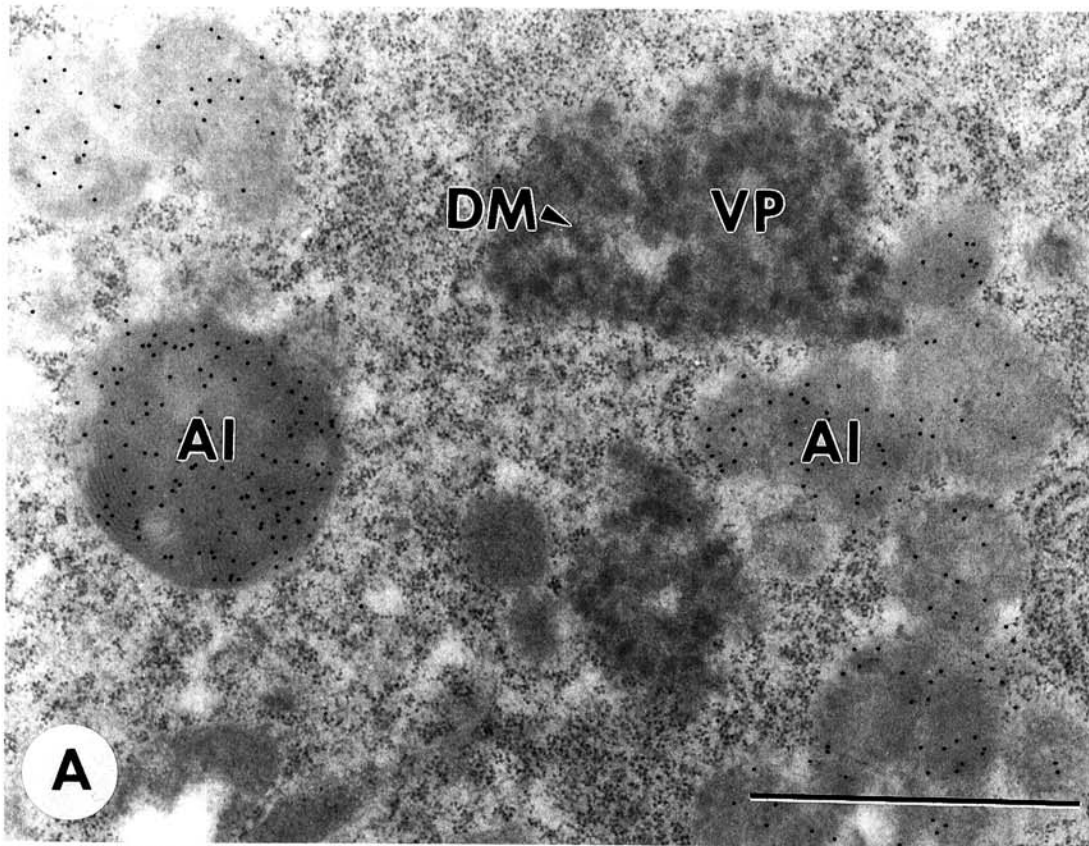


Fig. 2. Electron micrographs of serial thin sections of a larval thrips midgut epithelial cell showing compartmentalization of proteins in viral inclusions. Viroplasm with embedded electron-dense aggregates or dense masses abutting amorphous inclusions can be seen. Label is 15 nm Protein A-gold. Bars = 1 μ m. **(A)** Amorphous inclusions react with polyclonal antibody against the tomato spotted wilt tospovirus 78 kDa membrane glycoprotein while viroplasm and embedded dense masses do not. **(B)** Section serial to that shown in **(A)**. Viroplasm and dense masses react with polyclonal antibody against tomato spotted wilt tospovirus nucleocapsid protein while amorphous inclusions do not. AI, amorphous inclusion; DM, dense masses; VP, viroplasm.

ing was quantified by counting gold particles per cm^2 on structures (i.e., inclusions, vesicles, vacuoles) in different regions of the cells (infected insects: 3 cell locations per inclusion type \times 3 cell regions \times 2 insects \times 2 replications = 36 counts/inclusion type from 4 insects; noninfected control insects: 3 cell locations per inclusion type \times 3 cell regions \times 1 insect \times 2 replications = 18 counts from 2 insects). This quantification was statistically analyzed as previously described (42). Because the background labeling was exceedingly low, statistical quantification was not done for anti-G2 labeling or on linear structures such as intercellular membranes and membranes thought to be part of the Golgi complex.

Thrips Acquisition and Transmission of TSWV. Two replications of the following experiments were conducted 1 month apart. First instar larval WFT from noninfected green bean pods were placed in acquisition units on groups of excised, TSWV-infected *E. sonchifolia* leaves, and allowed to feed for 48 h. Excised leaves were obtained from 3 to 5 infected plants per acquisition unit and 5 acquisition units were used per replication (5 units per replication \times 3 to 5 plants per unit \times 2 replications = 30 to 50 infected plants). Groups of 50 to 100 thrips were placed in each acquisition unit. Noninfected thrips, used as healthy controls in inoculation tests and microscopic analyses, were fed simultaneously on noninfected *E. sonchifolia* in a similar fashion. A subsample of these individuals were fed on 5% sucrose solution in distilled water under Parafilm membranes and used as controls in immunolabeling experiments. Second instar larvae were then randomly selected from acquisition units after 48 h of acquisition feeding and prepared for immunocytochemistry as described in the previous section. Immunocytochemical analyses were performed on dissected organs of WFT from these subsamples (6 insects per replication \times 2 replications = 12 insects). Remaining larvae were allowed to continue feeding on TSWV-infected leaves until pupation (48 h) and were then reared to adulthood on noninfected

green bean pods replaced daily. A subsample of 10 adult thrips were then prepared for immunocytochemistry as described for larvae. In addition, 9 adults were embedded in Spurr's as previously described (38). Insects that were osmicated and embedded in Spurr's could not be immunolabeled due to loss of TSWV protein antigenicity (42). Remaining adults were used to inoculate plants (*E. sonchifolia*).

RESULTS

Antibody specificity. Specificity of the antibodies used in immunolabeling is demonstrated by highly significant differences in gold label per cm^2 on morphologically distinct inclusions compared with surrounding cytoplasm, serum controls, and noninfected insect controls (Table 1) ($P < 0.0001$). No significant differences in gold label per cm^2 were found on cytoplasm of TSWV-infected and noninfected insects using rabbit or mouse serum controls.

Electron microscopic observations. Electron microscopic observations of larval WFT fed on TSWV-infected plants revealed spherical membrane-bound virions in the digestive tract immediately following acquisition feeding in all larvae sectioned (6 insects per replication \times 2 replications = 12 insects) (Fig. 1). In infected larvae and adults four morphologically distinct, non-membrane-bound cytoplasmic inclusions were associated with TSWV structural and nonstructural proteins: viroplasm, dense masses, amorphous inclusions, and fibrous paracrystalline arrays (Figs. 2A and B; 3A–D). Viroplasm consisted of amorphous matrix material. Frequently, dense masses appeared as embedded aggregates of more electron-dense material within the viroplasm (Figs. 2; 3A, C, and D; 4A) and were also found, although rarely, in the cytoplasm (Fig. 5). Serial sections revealed that viroplasms with embedded dense masses were frequently found adjacent to and abutting, but not overlapping amorphous inclusions (Figs. 2A

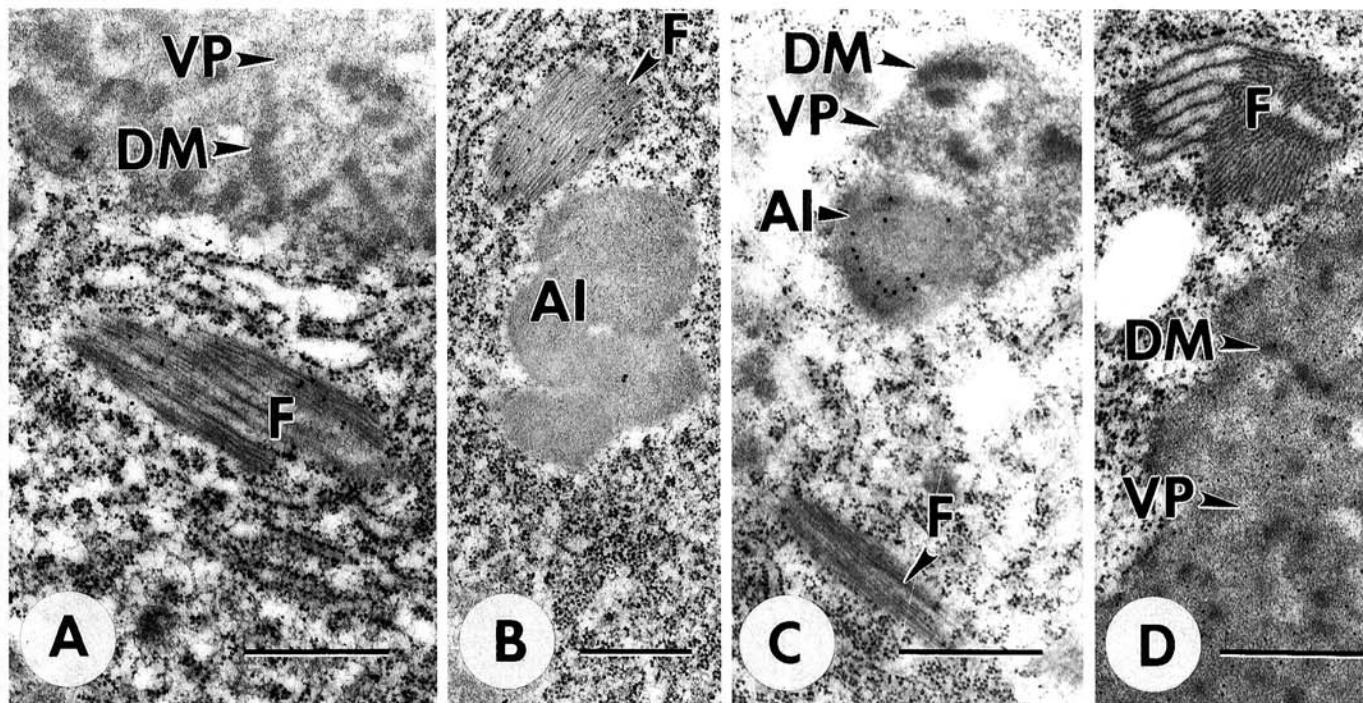


Fig. 3. Electron micrographs of thin sections of larval thrips midgut epithelial cells. Bars = 0.5 μm . (A) Fibrous paracrystalline array and viroplasm with embedded dense masses. Paracrystalline array reacts with polyclonal antibody to tomato spotted wilt tospovirus (TSWV) nonstructural protein encoded by the S RNA (NSs) while viroplasm and embedded dense masses do not. Label is 15 nm goat anti-rabbit-gold (GAR). (B) Paracrystalline array reacts with anti-NSs polyclonal antibodies while amorphous inclusion does not. Label is 15 nm GAR. (C) Viroplasm with embedded dense masses abutting an amorphous inclusion adjacent to a fibrous paracrystalline array. Amorphous inclusion reacts with polyclonal antibody to TSWV 78 kDa membrane glycoprotein while viroplasm, dense masses and fibrous paracrystalline array do not. Label is 15 nm Protein A-gold (PAG). (D) Viroplasm with embedded dense masses adjacent to a fibrous, paracrystalline array. Viroplasm and dense masses react with antibodies against TSWV nucleocapsid protein while paracrystalline array does not. Label is 15 nm PAG. AI, amorphous inclusion; DM, dense masses; F, fibrous paracrystalline array; VP, viroplasm.

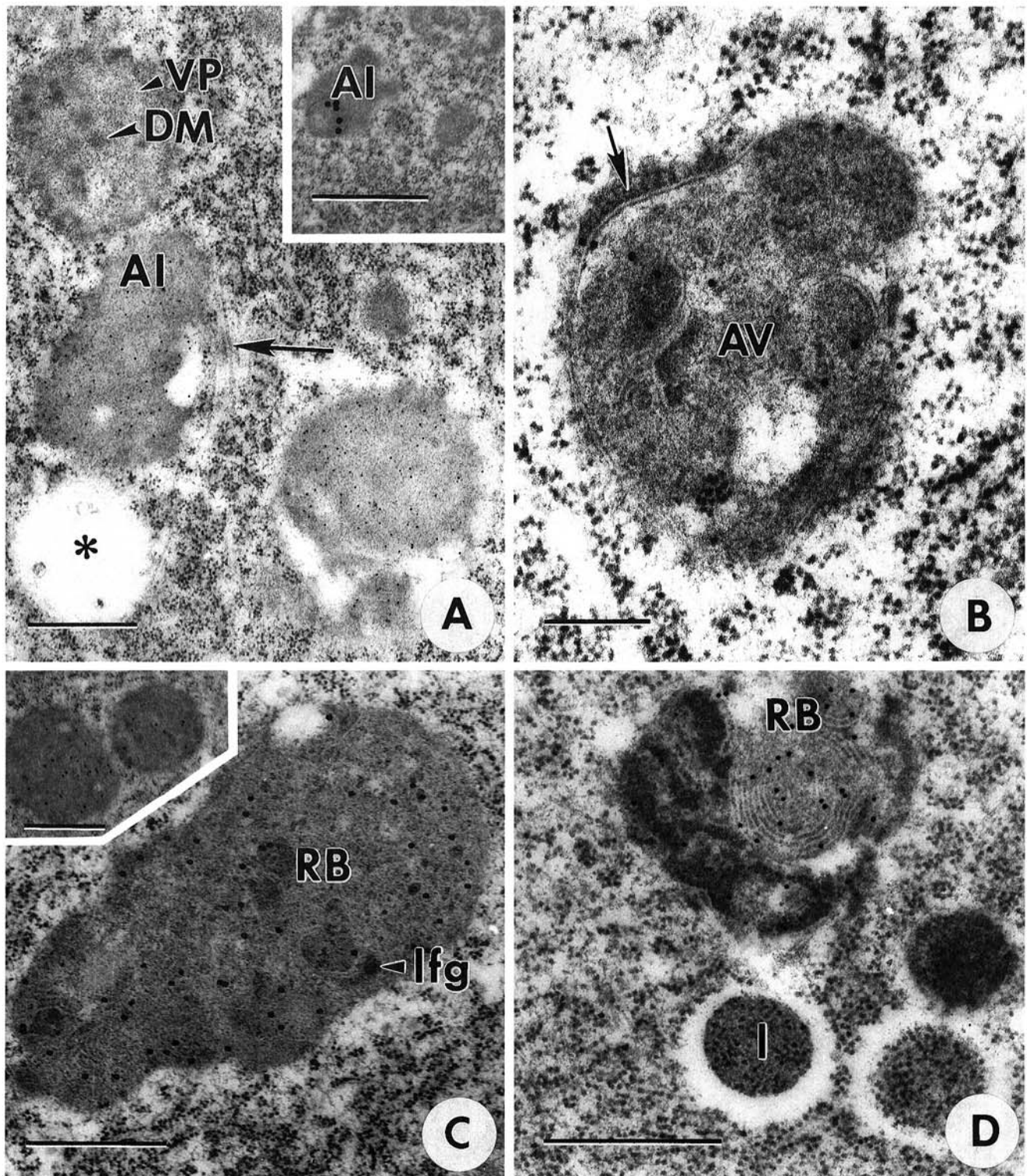


Fig. 4. Electron micrographs of thin sections of larval thrips midgut epithelial cells. (A) Viroplasm with embedded dense masses adjacent to amorphous inclusions. Area around amorphous inclusions is highly vacuolated (asterisk) and numerous microtubules are present adjacent to the inclusion and vacuolated region (arrow). Inset shows an amorphous inclusion. Amorphous inclusions react with antibodies against tomato spotted wilt tospovirus (TSWV) membrane glycoproteins (G1 in main photo, G2 in inset) while viroplasm and dense masses do not. Label on G1 is 10 nm Protein A-gold (PAG), whereas on G2 it is 15 nm silver enhanced PAG. Bars = 1 μ m. (B) Putative autophagic vacuole bounded by a distinctive double membrane. Contents are membranous, amorphous and electron dense. Electron dense material at cytosol edge (arrow) characterizes autophagic vacuoles. Bounding membrane and contents react with polyclonal antibodies against TSWV structural proteins. Label is 10 nm PAG. Bar = 0.2 μ m. (C) Putative residual bodies containing numerous membranous whorls, amorphous, electron dense materials and possible lipofuscin granules. Contents react with antibodies against TSWV G1 and G2 (G1 in main photo, G2 in inset). Label on G1 is 20 nm PAG, whereas label on G2 is 15 nm PAG. Bars = 0.5 μ m. (D) Residual body adjacent to a lysosome containing numerous membranous whorls and highly condensed electron dense material. Contents, particularly membranous whorls, react with polyclonal antibody against TSWV G1. Label is 15 nm PAG. Bar = 0.5 μ m. AI, amorphous inclusion; AV, autophagic vacuole; DM, dense masses; l, lysosome; lfg, lipofuscin granules; RB, residual body; VP, viroplasm.

and B; 3C; 4A). Amorphous inclusions consisted of amorphous, electron dense matrixes, often containing embedded membranous whorls (Fig. 2A). These inclusions frequently occurred next to large numbers of microtubules and were often vacuolated (Fig. 4A). Fibrous material in paracrystalline arrays occurred in various shapes and sizes throughout infected cells (Fig. 3A–D). Double enveloped particles, budding configurations in the Golgi apparatus and paired parallel membranes were not observed.

Virus-encoded proteins were also localized in vacuoles bound by a distinctive double membrane (provisionally named autophagic vacuoles based on their morphology) that occurred throughout the midgut epithelial cells of larvae (Figs. 4B; 5; 6A and B; 7), in residual bodies (Fig. 4C and D), in membranes thought to be part of the Golgi complex (Figs. 5; 8A and B), at intercellular membranes (Fig. 9A and B) and in smooth vesicles (Fig. 10). Among larvae, viroplasm, dense masses, and amorphous inclusions were seen in the midgut epithelial and muscle cells (replication 1: 5 of 6 insects sectioned; replication 2: 2 of 6 insects sectioned). Fibrous, paracrystalline arrays were found in the same cells, as well as autophagic vacuoles, residual bodies and smooth vesicles (in replication 1: 4 of 6 insects sectioned; in replication 2: 2 of 6 insects sectioned). Among infected adults (those reared on healthy beans following TSWV acquisition as larvae), viroplasms with embedded dense masses were observed in muscle cells surrounding the midgut in four of nine insects sectioned (Fig. 11), but not in the midgut epithelial cells. Viroplasms with embedded dense masses, fibrous, paracrystalline arrays and assembled virions were observed in the salivary gland of three of nine insects (Fig. 12). In virus transmission assays, the cohort from which these adults were subsampled successfully transferred TSWV to eight of 10 *E. sonchifolia* plants. Viroplasms with embedded dense masses, amorphous inclusions, paracrystalline arrays, and assembled virions were not seen in noninfected control insects. Putative autophagic vacuoles, residual bodies, and smooth vesicles were seen in control insects, but were less abundant than in infected insects.

Immunocytochemistry. Immunocytochemical analysis of serial ultrathin sections of larval and adult organs revealed that anti-N antibody reacted with virus particles (data not shown), viroplasm and dense masses (Figs. 2B; 3D; 5; 6A). In contrast, anti-

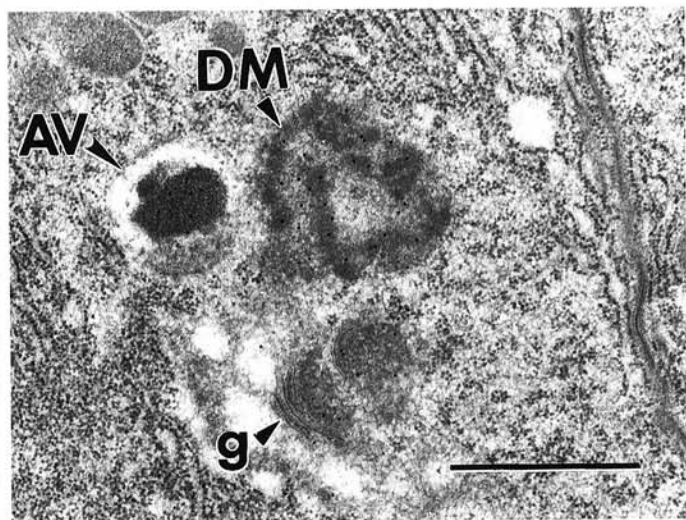


Fig. 5. Electron micrograph of a thin section of a larval thrips midgut epithelial cell showing dense masses in the cytoplasm rather than embedded in viroplasm. Dense masses are observed adjacent to an autophagic vacuole containing an accumulation of electron dense material. Dense masses, electron-dense material in the vacuole, and amorphous material adjacent to the Golgi are immunostained with polyclonal antibody against tomato spotted wilt tospovirus nucleocapsid protein. Label is 15 nm Protein A-gold. Bar = 1 μ m. AV, autophagic vacuole; DM, dense masses; g, Golgi.

bodies to G1 and G2 did not react with the viroplasm or dense masses, but did specifically tag virions (Fig. 1) (data not shown for G2) and amorphous inclusions (Figs. 2A; 3C; 4A). Fibrous, paracrystalline arrays were immunolabeled by anti-NSs antibodies (Fig. 3A and B), but did not react with anti-N or antibodies to G1 and G2 (Fig. 3C and D). Virions and inclusions were absent and immunolabel negligible (less than serum controls) (Table 1) in negative controls consisting of insects of the same age fed on noninfected plants.

In addition to cytoplasmic inclusions, autophagic vacuoles were found near viroplasms, dense masses and amorphous inclusions throughout the midgut epithelial cells of infected larvae (Figs. 4B; 5; 6A and B; 7). In some cases, vacuoles abutted viroplasms and amorphous inclusions, possibly fusing at the edge of these inclusions (Fig. 5). Vacuoles had distinctive double mem-

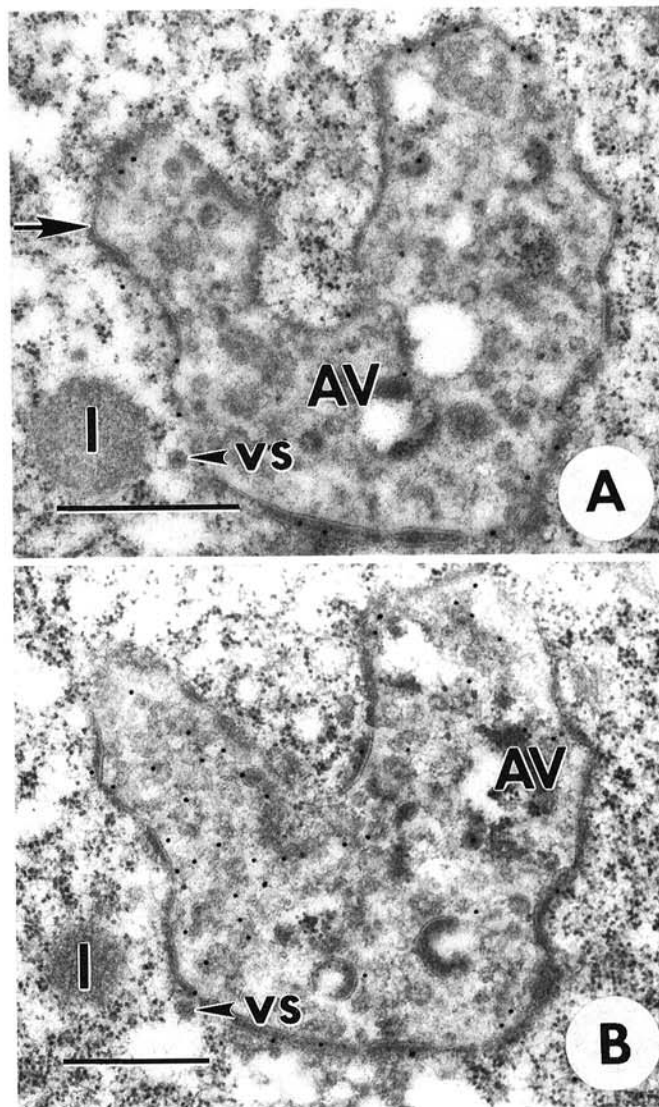


Fig. 6. Electron micrographs of serial thin sections of a larval thrips midgut epithelial cell revealing the protein composition of the contents of a putative autophagic vacuole. Bars = 0.5 μ m. (A) The autophagic vacuole is bounded by a distinct double membrane (arrow). Contents include amorphous, electron-dense material and membranous, vesicular material. A possible coated vesicle and lysosome can be seen adjacent to the vacuole membrane. The membrane bounding the vacuole and some of the contents are immunostained with polyclonal antibody against tomato spotted wilt tospovirus (TSWV) nucleocapsid protein. Label is 15 nm Protein A-gold (PAG). (B) Section serial to that shown in (A). Membrane bounding the vacuole and contents are immunostained with polyclonal antibody against the TSWV 78 kDa membrane glycoprotein (G1). Label is 15 nm PAG. AV, autophagic vacuole; vs, vesicle; l, lysosome.

branes (Fig. 6A and B) and the vacuole contents included membranous bits, whorls, spheres, and amorphous electron-dense materials (Figs. 4B; 6A and B; 7). The cytosol side of the vacuole membrane frequently had electron-dense deposits (Fig. 4B) similar to those occurring when clathrin are deposited following fusion between vacuoles and coated vesicles (Fig. 6A and B). Immunolabeling of serial sections revealed that the membrane bounding the vacuoles, as well as some of the vacuole contents, reacted with anti-N and antibodies to G1 and G2 (Figs. 5; 6A and B; 7), but were not tagged by anti-NSs antibodies (data not shown). Autophagic vacuoles containing virus encoded proteins were also observed along the basal and intercellular plasma membranes and apparently fused with the labyrinth of basal laminae infoldings at the basement membrane of the midgut epithelial cells (Fig. 7). Autophagic vacuoles in noninfected control larvae did not immunolabel with any of the antibodies used in this investigation.

Residual bodies were found in midgut epithelial cells of TSWV-infected larvae that reacted specifically with anti-G1 and

anti-G2 antibodies (Fig. 4C and D), but did not react with anti-N or anti-NSs antibodies. Anti-N and antibodies to G1 and G2 also tagged membranes of the Golgi complex (Fig. 8A and B), sections of the zonula continua (a junctional specialization of the intercellular membrane separating midgut epithelial cells) (Fig. 9A) and sections of the midgut epithelial cell basement membrane abutting circular and longitudinal muscle cells containing viroplasm with embedded dense masses (data not shown). Fibrous, paracrystalline arrays apparently spanning intercellular membranes reacted with anti-NSs antibody (Fig. 9B).

DISCUSSION

Our observations indicate that multiplication of TSWV in thrips cells results in viral proteins compartmentalized in cytoplasmic inclusions and localized at intercellular membranes and membranes thought to be part of the Golgi complex. In addition, viral proteins were found in various vesicles and vacuoles associated with autophagic pathways indicating that intracellular

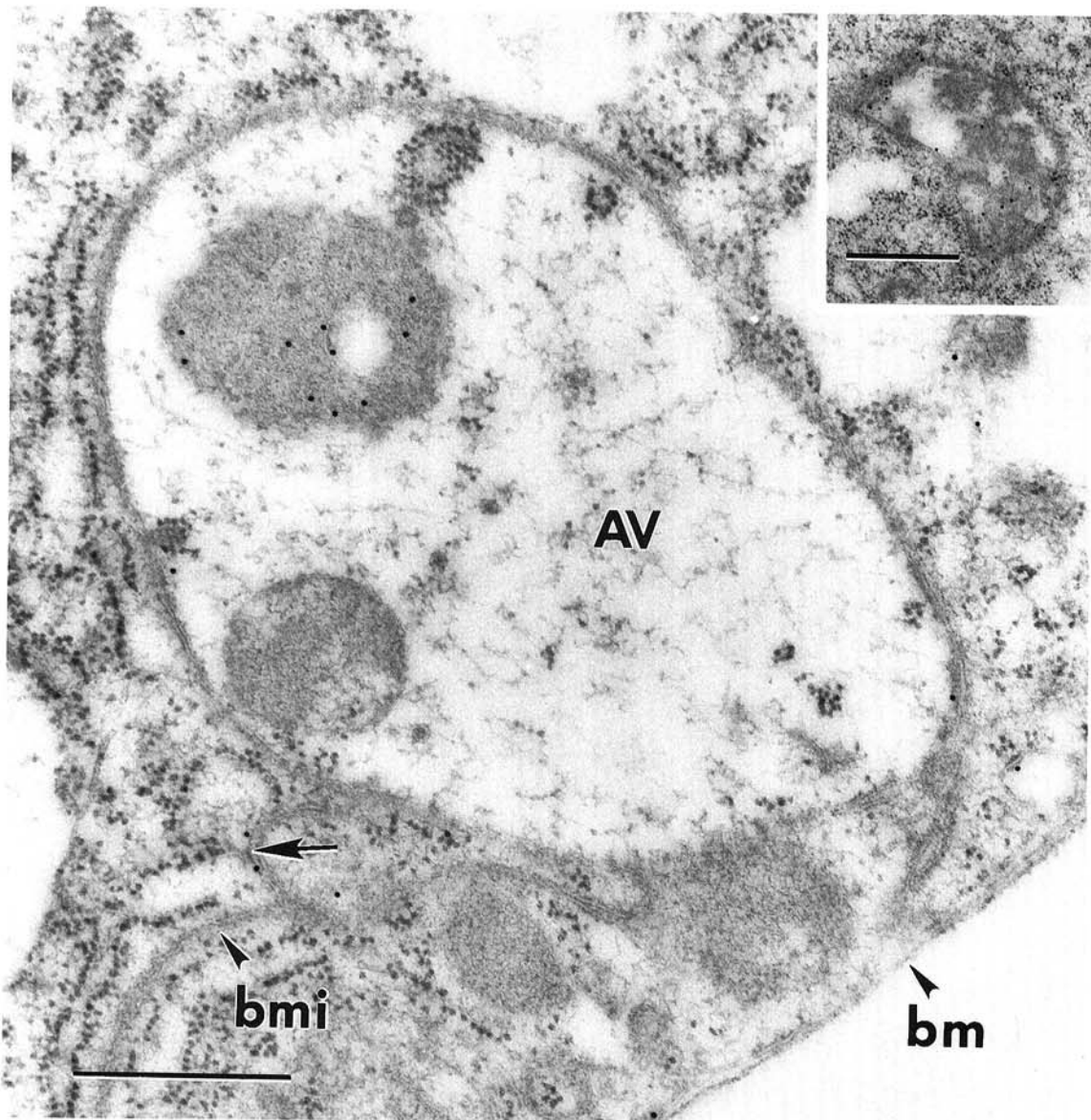


Fig. 7. Electron micrograph of a thin section of a larval thrips midgut epithelial cell showing a putative autophagic vacuole possibly fusing to an infolding of the basement membrane. Possible residual body within the vacuole and a portion of the basement membrane infolding (arrow) are immunostained with polyclonal antibody against tomato spotted wilt tospovirus (TSWV) 78 kDa membrane glycoprotein (G1) Bar = 0.5 μ m. Inset shows a putative autophagic vacuole immunostained with monoclonal antibody to the TSWV 58 kDa membrane glycoprotein (G2). Bar = 1 μ m. Label in main photo and inset is 15 nm Protein A-gold. AV, autophagic vacuole; bmi, basement membrane infolding; bm, basement membrane.

transport takes place in thrips in response to infection by TSWV.

The conclusion that viral N, G1, G2, and NSs proteins are compartmentalized in cytoplasmic inclusions is supported by immunolabeling of serial sections from infected thrips cells. Immunolabeling indicated that the viroplasm and dense masses were composed predominantly of N protein and not viral membrane glycoproteins or NSs (Figs. 2B; 3A and D; 4A; 8A). This confirms previous findings in plants infected with TSWV or INSV, in which the viroplasm and dense masses have also been shown to

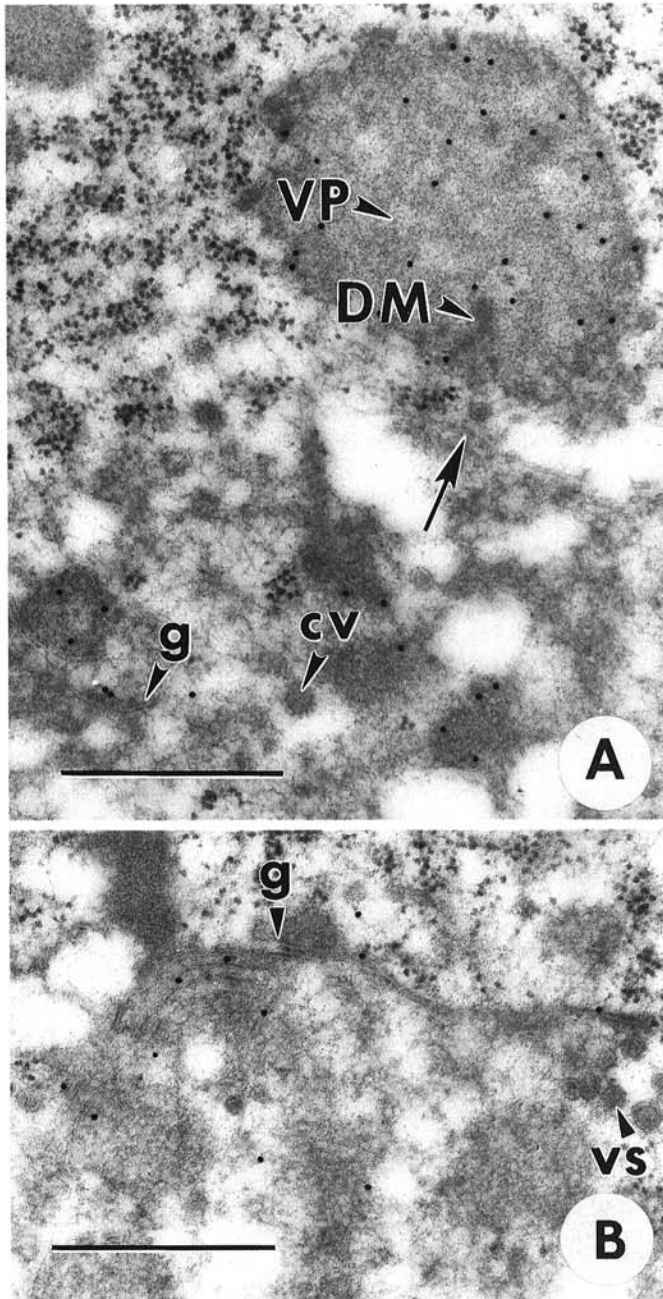


Fig. 8. Electron micrographs of thin sections of a larval thrips midgut epithelial cell. Label is 15 nm Protein A-gold. Bars = 0.5 μ m. (A) Putative Golgi region adjacent to a viroplasm with embedded dense masses. Numerous coated vesicles and microtubules (arrow) can be seen. Viroplasm, dense masses, and amorphous material in the Golgi region are immunostained with polyclonal antibodies against the tomato spotted wilt tospovirus (TSWV) nucleocapsid protein. (B) Putative Golgi region several serial sections after that shown in (A) immunostained with polyclonal antibody against the TSWV 78 kDa membrane glycoprotein (G1). Many vesicles can be seen in the region. cv, coated vesicle; DM, dense masses; g, Golgi; vs, vesicle; VP, viroplasm.

accumulate N protein (18,20,39). Amorphous inclusions were found adjacent to the viroplasm and embedded dense masses (Figs. 2A; 3C; 4A). In these inclusions TSWV membrane glycoproteins accumulated, but not the N or NSs proteins. In serial sections of viroplasms with embedded dense masses and amorphous inclusions, even when these inclusions were adjacent and

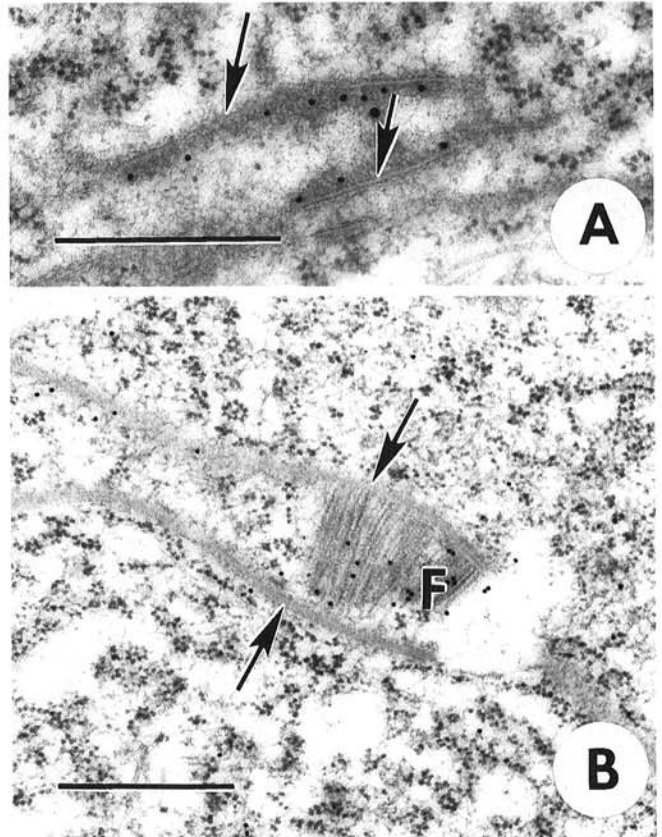


Fig. 9. Electron micrographs of thin sections of a larval thrips midgut epithelial cell. Bars = 0.5 μ m. (A) Amorphous, electron dense material along intercellular membranes (arrows) immunostained with polyclonal antibody against tomato spotted wilt tospovirus (TSWV) nucleocapsid protein. Label is 15 nm Protein A-gold. (B) Fibrous, paracrystalline array immunostained with antibody against TSWV nonstructural protein encoded by the S RNA spanning intercellular membranes (arrows). Label is 15 nm goat anti-rabbit gold. F, fibrous, paracrystalline array.

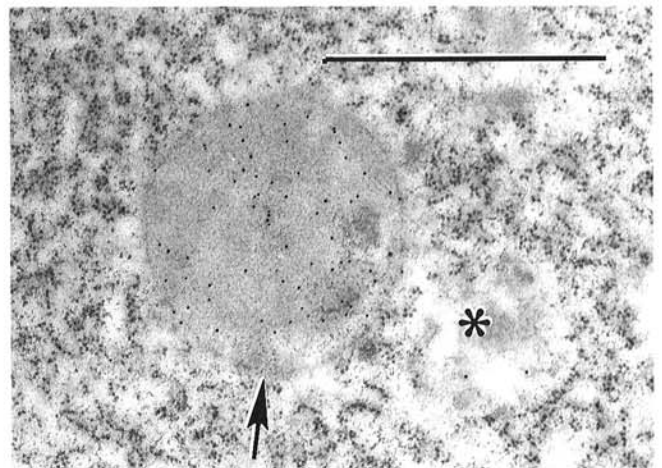


Fig. 10. Electron micrograph of a thin section of a larval thrips midgut epithelial cell showing a possible storage or transport vacuole (arrow) immunostained with polyclonal antibody against the tomato spotted wilt tospovirus 78 kDa membrane glycoprotein (G1). An adjacent vesicle (asterisk) immunolabels. Label is 10 nm Protein A-gold. Bar = 0.5 μ m.

abutting one another, the viral proteins were found compartmentalized. This suggests that viroplasm and amorphous inclusions may be parts of a single compartmentalized structure.

Although glycoproteins previously have been shown to occur in mature virions in plant cells and partially purified preparations (10,18) this is the first reported use of immunolabeling to indicate that amorphous inclusions are composed of membrane glycoproteins in insect or plant cells infected with TSWV. An amorphous inclusion was reported in plant cells infected with INSV, however, it did not label with antibodies to TSWV N and G2 (39). The composition was not further determined (39) and we do not know whether INSV induced amorphous inclusions are related to the amorphous inclusions we observe in infected thrips.

The NSs protein is compartmentalized in fibrous, paracrystalline arrays (Figs. 3A and B), but the N, G1, and G2 proteins were not detected in these inclusions. These observations affirm previous research documenting that the NSs protein is found solely in fibrous, paracrystalline arrays in insect cells, and not in the cytoplasm, viroplasm, dense masses, or amorphous inclusions (18, 31). These findings differ from those of Wijkamp et al. (43), in which NSs was localized in the cytoplasm of some thrips cells, as well as in fibrous, paracrystalline arrays. This difference may be related to variation in virus isolate, as NSs production does apparently vary with isolate (18,20), variation in thrips populations and their response to TSWV infection, or with variations in the time at which viral replicative events were documented. The role of NSs in the replicative process in thrips and plants remains unknown; however, the presence of this protein in thrips midguts, muscle cells, and salivary glands affirms previous findings that TSWV replicates in all these thrips cells (36,42,43).

The conclusion that viral N, G1, and G2 proteins may be transported to the Golgi complex is supported by the immunolabeling of these proteins at membranes thought to be part of the Golgi complex (Fig. 8A and B). Designation of these membranes as part of the Golgi complex is based on their morphology, including their configuration in serial sections, stacked appearance, and the large number of coated vesicles occurring nearby (26). The structural resolution of membranes in these immunolabeled ultra-

thin sections is less distinct than it would be if the specimens had been osmicated and embedded in Spurr's resin; however, these treatments are not compatible with immunolabeling because they destroy the antigenicity of TSWV (42). Similar membrane configurations were observed in noninfected thrips that had been osmicated and embedded in Spurr's. Therefore, it is our contention that these membrane configurations are part of the Golgi complex and not TSWV-induced structures. Membrane glycoproteins of other viruses in the family *Bunyaviridae* have been localized specifically in the membranes of the Golgi complex where they are thought to accumulate prior to virus maturation (6,8,22, 28,30,31,41). The Golgi complex has been suggested as a site of TSWV maturation based on analogy to other viruses in the family *Bunyaviridae* (18) and configurations in the Golgi of TSWV-infected plants that have been interpreted as membranes budding to form particles (24). This is the first report providing serological evidence that TSWV-encoded proteins are associated with membranes thought to be part of the Golgi complex of infected plant or insect cells. We cannot ascertain whether the proteins we are labeling were produced de novo during TSWV replication or entered the cell during virus endocytosis and are being processed in the Golgi complex (26). However, if the proteins in the Golgi complex were produced de novo, they may be accumulating prior to virus maturation providing evidence toward support of a model in which the Golgi is the site of TSWV maturation. We have not observed the process of virion maturation in thrips cells; however, our data represent a first step toward defining the events leading to virion maturation in thrips cells.

The function and/or fate of TSWV-encoded proteins accumulating in inclusions has not been elucidated. It has been suggested

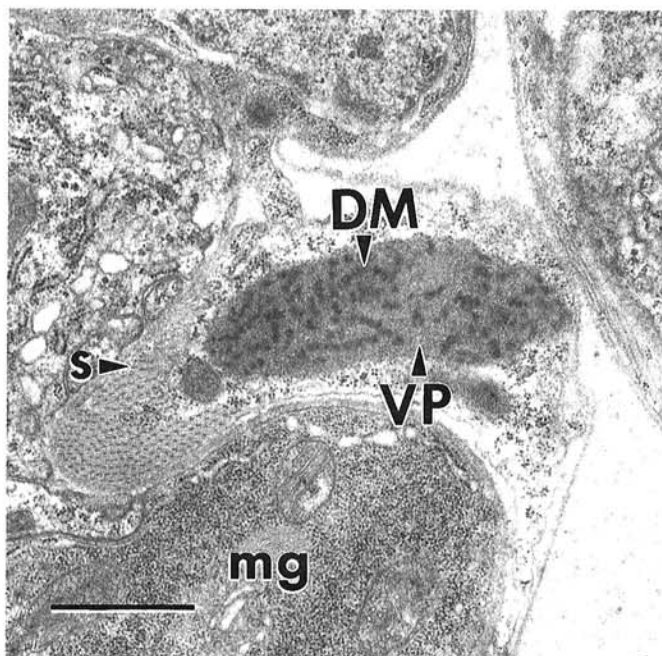


Fig. 11. Electron micrograph of a thin section of an adult thrips muscle cell showing a viroplasm with embedded dense masses within the cell. Adjacent midgut epithelial cells can also be seen. Bar = 1 μ m. DM, dense masses; mg, midgut epithelial cell; s, cross section of striated muscle; VP, viroplasm.

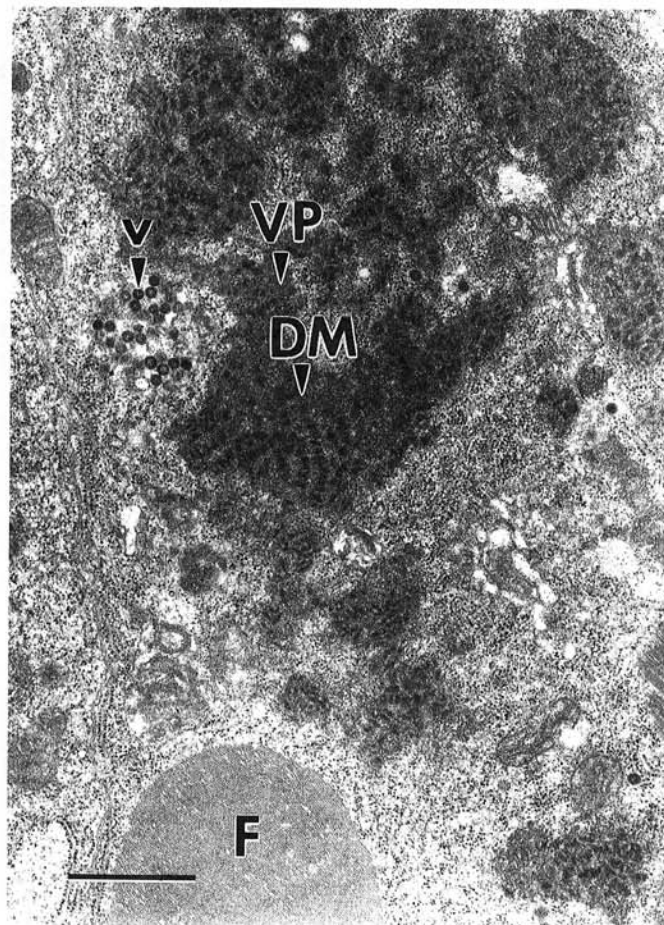


Fig. 12. Electron micrograph of a thin section of an adult thrips salivary gland cell showing cytoplasmic inclusions and mature virions. Bar = 1 μ m. DM, dense masses; F, fibrous paracrystalline array; v, virions; VP, viroplasm.

for other plant viruses, such as cauliflower mosaic virus, that inclusions may have a role in the viral replication cycle and may serve as centers of degradation for viral proteins (29). While it seems likely that TSWV-encoded proteins that are compartmentalized in inclusions in thrips cells may have more than one fate, we found these proteins in putative autophagic structures where they could be degraded and exocytosed. Putative autophagic vacuoles containing TSWV N, G1, and G2 proteins were found near inclusions and possibly fusing at the edges of inclusions. Thus, the vacuoles could acquire proteins directly from inclusions. In addition, autophagic vacuoles containing TSWV proteins apparently fuse with infoldings of the basal membrane of the midgut cells (Fig. 7). This indicates that proteins may be exocytosed through the basal membrane.

The morphology of the vacuoles strongly supports their role in autophagy. They are bound by a distinctive double membrane characteristic of autophagic vacuoles (Figs. 4B; 6A and B) (4,15, 26,27). The electron-dense deposits on the cytosol edge of the bounding membrane (Fig. 4B) are characteristic of the presence of clathrin, the protein that coats coated vesicles, remaining at the membrane surface (14). In serial sections, the vacuoles appeared fused with coated vesicles (Fig. 6A and B), which is characteristic of autophagic vacuoles because proteins designated for removal from the cytoplasm and degradative enzymes are delivered to the vacuole by continuous fusing with coated vesicles (14). After coated vesicles fuse with vacuoles, the clathrin coating of the vesicles is often left at the surface of the receiving vacuole leaving an electron-dense deposit on the cytosol side of the vacuole membrane (15). Presence of viral N, G1, and G2 proteins in autophagic vacuoles suggests that these proteins are transported intracellularly, degraded, and possibly exocytosed from the cell via these subcellular structures. Other vesicles that may be storing proteins or moving them intracellularly are also common and can be seen adjacent to autophagic vacuoles (Fig. 10). Thus, TSWV proteins appear to be transported around the cell in a variety of ways and proteins may be delivered to autophagic vacuoles by several agents of the cell's internal transport system. Similar autophagic vacuoles that did not immunolabel were found in noninfected control insects. This shows that these structures are not endomembrane systems induced by virus infection, as is postulated for double enveloped virions and paired parallel membranes (24). Instead these structures are part of the cell's normal autophagic system. As would be expected, the abundance of autophagic vacuoles in infected thrips is greater than in noninfected control insects. This outcome is logical because the autophagic system is part of the cell's defense against accumulation of foreign proteins and this system is known to fluctuate in response to altered physiological states (15,26,44).

Additional evidence that TSWV proteins enter the cell's autophagic system is provided by finding residual bodies containing viral G1 and G2 proteins (Fig. 4C and D) in infected midgut epithelial cells. Residual bodies are thought to be a degradative endpoint for proteins entering a cell's autophagic system (15). There may be more than one autophagic pathway involved in degradation of TSWV proteins as only TSWV membrane glycoproteins were detected in residual bodies while viral N, G1, and G2 proteins were detected in autophagic vacuoles. The amorphous inclusions in which viral glycoproteins were compartmentalized were often filled with membranous whorls similar to those later seen in residual bodies. Amorphous inclusions were also frequently highly vacuolated and associated with microtubules indicating association with the cell's internal transport system (Fig. 4A). Some of these amorphous inclusions may be in the early stages of processing that results in residual body formation. Residual bodies, autophagic vacuoles, and Golgi processing of foreign proteins are all stages in the dynamic process of protein digestion and membrane turnover that occurs in cells (15,26,27), and thus, these subcellular structures may be part of a thrips cell

response to accumulation of viral proteins. Autophagy has not been previously shown in insect vector cells infected with a virus that is also pathogenic to plants nor have any of the other viruses in the family *Bunyaviridae* been shown to cause cytopathology in their vectors (13). This information also supports the hypothesis that TSWV is pathogenic in both its animal and plant hosts.

The functions of viroplasm, amorphous inclusions, and paracrystalline arrays are unknown. However, their presence in thrips midguts, muscle cells, and salivary glands indicates that TSWV infection is widespread (Figs. 2–4; 11; 12). The detection of viral inclusions in the muscle cells of larvae after only 48 h of acquisition feeding shows that virus rapidly spreads from organ to organ. Virus movement from larval midguts was previously demonstrated after just 1 to 2 h of acquisition feeding (35) and viroplasm with embedded dense masses were detected in larval muscle cells after 24 h of acquisition feeding (43). Although TSWV infection in thrips is widespread and viral proteins are readily detected in cells, the only assembled virus particles observed in larvae are those present in the midgut lumen following ingestion from infected plants (Fig. 1). The lack of virions in cells when infection is widespread is unusual and contrasts with other viruses in the *Bunyaviridae*, in which infection results in production of mature virions that spread from cell to cell by exocytosis or budding at basal membranes (3,7,14,22,33). Our data suggest a different model, in which TSWV spreads from cell to cell as viral protein–RNA complexes and not as mature virions (36). The infections we observed occur in conjunction with production of mature virions in the salivary glands, and adults subsampled for plant inoculation successfully infected plants. Thus, our findings do not represent abortive or abnormal replicative processes. The pathway for replication and maturation of TSWV appears to be unique compared with other viruses in the family *Bunyaviridae* and with other plant viruses that replicate in insects. Future elucidation of the mechanisms underlying TSWV maturation and transport between thrips cells may lead to a better approach to managing the many diseases caused by this virus.

LITERATURE CITED

- Adkins, S. T., Quadt, R., Choi, T. J., Ahlquist, P., and German, T. L. 1995. An RNA-dependent RNA polymerase activity associated with virions of tomato spotted wilt virus, a plant- and insect-infecting bunyavirus. *Virology* 207:308-311.
- Bandla, M. D., Westcot, D. M., Chenault, K. D., Ullman, D. E., German, T. L., and Sherwood, J. L. 1994. Use of monoclonal antibody to the nonstructural protein encoded by the small RNA of tomato spotted wilt tospovirus to identify viruliferous thrips. *Phytopathology* 84:1427-1431.
- Booth, T. F., Gould, E. A., and Nuttall, P. A. 1991. Structure and morphogenesis of Dugbe virus (*Bunyaviridae*, *Nairovirus*) studied by immunogold electron microscopy of ultrathin cryosections. *Virus Res.* 21: 199-212.
- Bozzola, J. J., and Russell, L. D. 1992. *Electron Microscopy: Survey of Biological Ultrastructure*. Jones and Bartlett Publishers, Boston.
- Brittlebank, C. C. 1919. Tomato diseases. *J. Agric. Victoria Aust.* 17: 231-235.
- Chen, S. Y., and Compans, R. W. 1991. Oligomerization, transport and Golgi retention of Punta Toro virus glycoproteins. *J. Virol.* 65:5902-5909.
- Chen, S. Y., Matsuoka, Y., and Compans, R. W. 1991. Assembly and polarized release of Punta Toro virus and effects of brefeldin A. *J. Virol.* 65:1427-1439.
- Chen, S. Y., Matsuoka, Y., and Compans, R. W. 1991. Golgi complex localization of the Punta Toro virus G2 protein requires its association with the G1 protein. *Virology* 183: 351-365.
- Choi, T.-J., Chenault, K. D., Ullman, D. E., Sherwood, J. L., and German, T. L. 1993. Cloning and expression of the tomato spotted wilt virus (TSWV) NSm protein in *E. coli*. (Abstr.) *Phytopathology* 83:1425-1426.
- de Avila, A. C., Huguenot, C., Resende, R. d. O., Kitajima, E. W., Goldbach, R. W., and Peters, D. 1990. Serological differentiation of 20 isolates of tomato spotted wilt virus. *J. Gen. Virol.* 71:2801-2807.
- de Haan, P., Kormelink, R., Resende, R. d. O., van Poelwijk, F., Peters, D., and Goldbach, R. 1991. Tomato spotted wilt virus L RNA encodes a putative RNA polymerase. *J. Gen. Virol.* 71:2207-2216.
- de Haan, P., Wagemakers, L., Goldbach, R., and Peters, D. 1989. Tomato

- spotted wilt virus, a new member of the Bunyaviridae? Pages 287-290 in: Pathogenicity of Negative Strand Viruses. D. Kolakofsky, ed. Elsevier, Amsterdam.
13. de Haan, P., Wagemakers, L., Peters, D., and Goldbach, R. 1990. The S RNA segment of tomato spotted wilt virus has an ambisense character. *J. Gen. Virol.* 71:1001-1007.
 14. Elliott, R. M. 1990. Molecular biology of the bunyaviridae. *J. Gen. Virol.* 71:501-522.
 15. Fawcett, D. W. 1981. Lysosomes, Pages 487-514 in: *The Cell*. W. B. Saunders Co. Philadelphia.
 16. Francki, R. I. B., and Grivell, C. J. 1970. An electron microscope study of the distribution of tomato spotted wilt virus in systemically infected *Datura stramonium* leaves. *Virology* 42:969-978.
 17. German, T. L., Ullman, D. E., and Moyer, J. W. 1992. Tospoviruses: Diagnosis, molecular biology, phylogeny, and vector relationships. *Ann. Rev. Phytopathol.* 30:315-348.
 18. Kitajima, E. W., de Avila, A. C., Resende, R. d. O., Goldbach, R., and Peters, D. 1992. Comparative cytological and immunogold labeling studies on different isolates of tomato spotted wilt virus. *J. Submicrosc. Cytol. Pathol.* 24:1-14.
 19. Kormelink, R., de Haan, P., Meurs, C., Peters, D., and Goldbach, R. 1992. The nucleotide sequence of the M RNA segment of tomato spotted wilt virus, a bunyavirus with two ambisense RNA segments. *J. Gen. Virol.* 73:2795-2804.
 20. Kormelink, R., Kitajima, E. W., de Haan, P., Zuidema, D., Peters, D., and Goldbach, R. 1991. The nonstructural protein (NSs) encoded by the ambisense S RNA segment of tomato spotted wilt virus is associated with fibrous structures in infected plant cells. *Virology*. 181:459-468.
 21. Kormelink, R., Storms, M., Van Lent, J., Peter, D., and Goldbach R. 1994. Expression and subcellular location of NSm protein of tomato spotted wilt virus (TSWV), a putative viral movement protein. *Virology* 200:56-65.
 22. Matsuoka, S. Y., and Compans, R. W. 1991. Bunyavirus protein transport and assembly, Pages 161-179 in: *Current Topics in Microbiology and Immunology*. D. Kolakofsky, ed., Springer-Verlag, Berlin.
 23. Mau, R. F. L., Bautista, R., Cho, J. J., Ullman, D. E., Gusukuma Minuto, L., and Custer, D. M. 1990. Factors affecting the epidemiology of TSWV in field crops: Comparative virus acquisition efficiency of vectors and suitability of alternate hosts to *Frankliniella occidentalis* (Pergande). *Virus-Thrips-Plant Interaction of Tomato Spotted Wilt Virus*, Proc. USDA Worksh. ARS-87:21-27.
 24. Milne, R. G. 1970. An electron microscope study of tomato spotted wilt virus in sections of infected cells and in negative stain preparations. *J. Gen. Virol.* 6:267-276.
 25. Milne, R. G., and Francki, R. I. B. 1984. Should tomato spotted wilt virus be considered as a possible member of the family Bunyaviridae? *Intervirology* 22:72-76.
 26. Pastan, I., and Willingham, M. C. 1985. The pathway of endocytosis. Pages 1-15 in: *Endocytosis*. I. Pastan, ed. Plenum Press. New York.
 27. Pastan, I. H., and Willingham, M. C. 1981. Journey to the center of the cell: Role of the receptosome. *Science* 214:504-509.
 28. Persson, R., and Pettersson, R. F. 1991. Formation and intracellular transport of a heterodimeric viral spike protein complex. *J. Cell Biol.* 112(2):257-266.
 29. Reinke, K. J., and de Zoeten, G. A. 1991. *In situ* localization of plant viral gene products. *Phytopathology* 81:1306-1314.
 30. Ronnholm, R. 1992. Localization to the Golgi complex of Uukuniemi virus glycoproteins G1 and G2 expressed from cloned cDNAs. *J. Virol.* 66:4525-4531.
 31. Ruusala, A., Persson, R., Schmaljohn, C. S., and Pettersson, R. F. 1992. Coexpression of the membrane glycoproteins G1 and G2 of Hantaan virus is required for targeting to the Golgi complex. *Virology* 186:53-64.
 32. Samuel, G., Bald, J. G., and Pittman, H. A. 1930. Investigations on "spotted wilt" of tomatoes in Australia. *Commonw. Coun. Sci. Ind. Res. Bull.* No. 44.
 33. Schmaljohn, C. S., and Patterson, J. L. 1990. Bunyaviridae and their replication: Part II. Replication of bunyaviridae. In: *Fields Virology*. B. N. Fields and D. M. Knipe, eds. Raven, New York.
 34. Sherwood, J. L., Sanborn, M. R., and Keyser, G. C. 1987. Production of monoclonal antibodies to peanut mottle virus and their use in enzyme-linked immunosorbent assay and dot-immunobinding assay. *Phytopathology* 77:1158-1161.
 35. Ullman, D. E., Cho, J. J., Mau, R. F. L., Westcot, D. M., and Custer, D. M. 1992. A midgut barrier to tomato spotted wilt virus acquisition by adult western flower thrips. *Phytopathology* 82: 1333-1342.
 36. Ullman, D. E., German, T. L., Sherwood, J. L., Westcot, D. M., and Cantone, F. A. 1993. *Tospovirus* replication in insect vector cells: Immunocytochemical evidence that the nonstructural protein encoded by the S RNA of tomato spotted wilt tospovirus is present in thrips vector cells. *Phytopathology* 83:456-463.
 37. Ullman, D. E., Sherwood, J. L., German, T. L., Westcot, D. M., Chenualt, K. D., and Cantone, F. A. 1993. Location and composition of cytoplasmic inclusions in thrips cells infected with tomato spotted wilt tospovirus (TSWV). (Abstr.) *Phytopathology* 83:1374.
 38. Ullman, D. E., Westcot, D. M., Hunter, W. B., and Mau, R. F. L. 1989. Internal anatomy and morphology of *Frankliniella occidentalis* (Pergande) (Thysanoptera: Thripidae) with special reference to interactions between thrips and tomato spotted wilt virus. *Int. J. Insect Morphol. Embryol.* 18:289-310.
 39. Urban, L. A., Huang, P.-Y., and Moyer, J. W. 1991. Cytoplasmic inclusions in cells infected with isolates of L and I serogroups of tomato spotted wilt virus. *Phytopathology* 81:525-529.
 40. Wang, M., and Gonsalves, D. 1990. ELISA detection of various tomato spotted wilt virus isolates using specific antisera to structural proteins of the virus. *Plant Disease* 74:154-158.
 41. Wasmoen, R. L., Kalach, L. T., and Collett, M. S. 1988. Rift Valley Fever virus M segment: Cellular localization of M segment-encoded proteins. *Virology* 166:275-280.
 42. Westcot, D. M., Ullman, D. E., Sherwood, J. L., Cantone, F. A., and German, T. L. 1993. Rapid fixation and embedding method for immunocytochemical studies of tomato spotted wilt tospovirus (TSWV) in plant and insect tissues. *Microscopy Research and Technique* 24:514-520.
 43. Wijkamp, I., van Lent, J., Kormelink, R., Goldbach, R., and Peters, D. 1993. Multiplication of tomato spotted wilt virus in its insect vector, *Frankliniella occidentalis*. *J. Gen. Virol.* 74:341-349.
 44. Willingham, M. C., and Pastan, I. 1980. The receptosome: An intermediate organelle or receptor-mediated endocytosis in cultured fibroblasts. *Cell* 21:67-77.